



## A novel pyridinium hemicyanine dye with carboxylate anchoring group and its application in dye-sensitized solar cells

Yifan Shan<sup>a</sup>, Jie Tang<sup>a</sup>, Hua Lai<sup>b</sup>, Hongwei Tan<sup>c</sup>, Fan Yang<sup>a,\*</sup>, Qiang Fang<sup>b,\*</sup>, Pierre Audebert<sup>d</sup>, Adam Pron<sup>e</sup>

<sup>a</sup>Institutes for Advanced Interdisciplinary Research, East China Normal University, Shanghai 200062, China

<sup>b</sup>Shanghai Institute of Organic Chemistry, Chinese Academy of Sciences, Shanghai 200032, China

<sup>c</sup>Department of Chemistry, Beijing Normal University, Beijing 100875, China

<sup>d</sup>P. P. S. M., UMR 8531, Ecole Normale Supérieure de Cachan, 94235 CACHAN, France

<sup>e</sup>CEA Grenoble INAC/SPRAM (UMR 5819), 17 Rue des Matyrès 38 38054 Grenoble, France

### ARTICLE INFO

#### Article history:

Received 28 October 2011

Revised 26 December 2011

Accepted 30 December 2011

Available online 16 January 2012

### ABSTRACT

A novel organic dye with N-substituted pyridinium as the acceptor and carboxylate as the anchoring group were designed and synthesized for dye-sensitized solar cells, which give solar energy-to-electricity conversion efficiency ( $\eta$ ) of up to 3.47% in comparison with the reference Ru-complex (N719 dye) with an  $\eta$  value of 5.27% under similar experimental conditions. This new dye is simple in structure, very easy to synthesize, and gives high  $V_{oc}$ .

© 2012 Elsevier Ltd. All rights reserved.

Dye-sensitized solar cells (DSSCs) using ruthenium based dyes have been actively investigated since Grätzel and co-workers reported the first case of a highly efficient photovoltaic device with the conversion efficiencies up to 11% at standard AM1.5 sun light.<sup>1–7</sup> Compared with ruthenium based dyes, metal-free organic dyes exhibit higher molar extinction coefficients, and more importantly they can be prepared and purified in simpler procedures at lower cost. Therefore, the development of novel metal-free organic dyes to achieve high solar to electric power conversion efficiencies has attracted more and more attention. Great advance in the use of organic dyes for DSSCs has been made recently. A variety of organic dyes such as coumarin dyes,<sup>8,9</sup> hemicyanine dyes,<sup>10,11</sup> indoline dyes,<sup>12–14</sup> merocyanine dyes,<sup>15</sup> triphenylamine-based dyes<sup>16–19</sup> and et al have been developed. It is very instructive that porphyrin-sensitized solar cells with cobalt (II/III)-based redox electrolyte can achieve 12.3% efficiency according to the report of Grätzel and co-workers<sup>24</sup> in 2011. The most efficient hemicyanine dyes for DSSCs have been reported so far are D- $\pi$ -A-type cationic dyes with *p*-dialkylaminophenyl groups as donors, cationic groups as acceptors such as benzo- and naphthothiazolium, pyridinium, and indolium salts, and methine anchoring groups. The overall yields were improved when the long alkyl chains were replaced by (–CH=CH–) units as  $\pi$  conjugation linkers between the donors and acceptors.<sup>20</sup> In 2000, Huang and co-workers reported pyridinium hemicyanine dyes PS and LPS with sulfonates (–SO<sub>3</sub><sup>–</sup>) as the methyl group.<sup>10</sup> Zhang and co-workers reported five new benzothiazolium

hemicyanine dyes with carboxylates as anchoring groups, which exhibited improved IPCEs and overall photoelectric conversion efficiencies in the DSSCs compared to the dyes with the same chromophores, but sulfonates as anchoring groups. It was found that TiO<sub>2</sub> absorbs carboxylates (–COO<sup>–</sup>) better than sulfonates (–SO<sub>3</sub><sup>–</sup>) and the interactions between TiO<sub>2</sub> and carboxylates are also stronger. Therefore, shorter tethering groups could be used to ensure closer contact between dyes and TiO<sub>2</sub>.<sup>21</sup>

The major problems for low conversion efficiency of many organic dyes in the DSSCs are the formation of dye aggregates on the semiconductor surface and recombination of conduction-band electrons with triiodide. However, these problems could be solved by using appropriate molecular structural design and modification.<sup>19</sup>

Herein, we report a new pyridinium hemicyanine dye (CP1) with carboxylate as anchoring group (Fig. 1). To the best of our knowledge, the application of these type of pyridinium acceptors in DSSCs has never been reported. CP1 can be easily synthesized with inexpensive materials and shows good efficiencies. CP1 molecule employs a diphenylamine moiety as the electron donor, a pyridinium moiety as the electron acceptor and a carboxylate as the anchoring group to attach to TiO<sub>2</sub> (see Fig. 1). The ethoxy-substituted oligo-phenylenevinylene chain extends the *p*-conjugation and thereby gives a red shift in the absorption spectrum without affecting the stability of the dye. The hemicyanine dye PS with sulfonate (–SO<sub>3</sub><sup>–</sup>) as the anchoring group<sup>10</sup>, which was reported by Huang and co-workers, is also synthesized for comparison.

The absorption, emission, and electrochemical properties of PS and CP1 are listed in Table 1. Absorption spectra of these dyes in CH<sub>2</sub>Cl<sub>2</sub> solutions at a concentration of 1 × 10<sup>–5</sup> M are shown in

\* Corresponding authors. Tel.: +86 21 62232764; fax: +86 21 62232100.

E-mail addresses: [fyang@chem.ecnu.edu.cn](mailto:fyang@chem.ecnu.edu.cn) (F. Yang), [qiangfang@mail.sioc.ac.cn](mailto:qiangfang@mail.sioc.ac.cn) (Q. Fang).

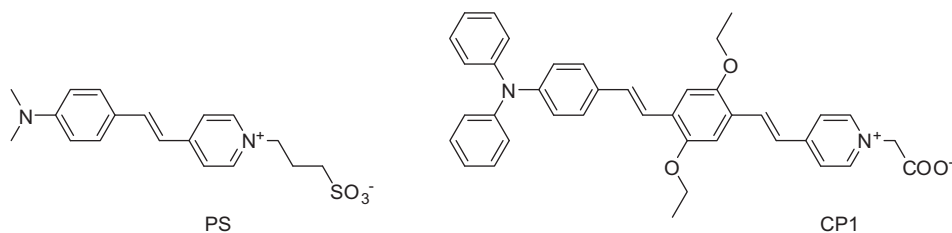


Figure 1. Chemical structures of PS and CP1.

Table 1  
Absorption, emission, and electrochemical properties of PS and CP1

Dye	Absorption <sup>a</sup>		Emission <sup>a</sup>		Oxidation potential data <sup>b</sup>		
	$\lambda_{\max}/\text{nm}$	$\epsilon/M^{-1}\text{cm}^{-1}$	$\lambda_{\text{em}}/\text{nm}$	$E_{0-0}/\text{V}$	$E_{\text{ox}}/\text{V}$	$E_{\text{ox}} - E_{0-0}/\text{V}$	
PS	514	46,100	601	2.21	0.90	-1.31	
CP1	519	36,400	663	2.12	1.09	-1.03	

<sup>a</sup> Absorption and emission spectra were measured in  $\text{CH}_2\text{Cl}_2$  solution ( $1 \times 10^{-5}$  M) at room temperature.

<sup>b</sup> The oxidation potentials of the dyes were measured in  $\text{CH}_2\text{Cl}_2$  with 0.1 M tetrabutylammonium hexafluorophosphate (TBAPF<sub>6</sub>) as electrolyte (working electrode: glassy carbon; reference electrode: Ag/AgCl/I<sup>-</sup>; calibrated with ferrocene/ferrocenium (Fc/Fc<sup>+</sup>) as an internal reference and converted to NHE by addition of 0.55 V, counter electrode: Pt).

<sup>c</sup>  $E_{0-0}$  was estimated from the onset point of absorption spectra.

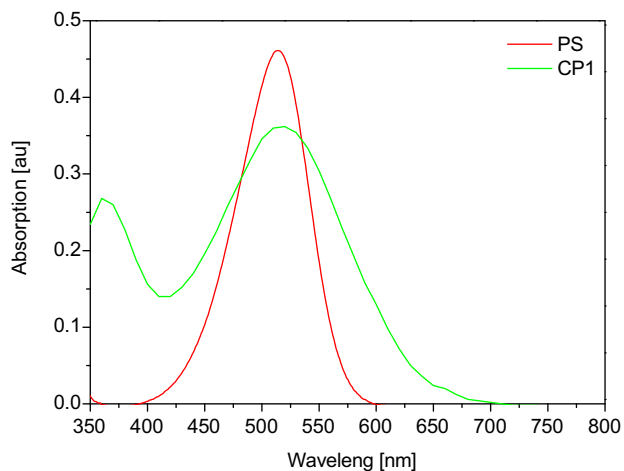


Figure 2. Absorption spectra of PS and CP1 in  $\text{CH}_2\text{Cl}_2$  solutions ( $1 \times 10^{-5}$  M).

Figure 2. Both PS and CP1 have relatively broad and strong absorptions in the visible region with maxima at 514 and 519 nm, respectively. CP1 has two intense absorption maxima at 363 and 519 nm, indicating  $\pi$ - $\pi^*$  transition and intramolecular charge transfer (ICT) between the donor and the pyridinium acceptor, respectively. The molar extinction coefficients of PS and CP1 are  $46,100 \text{ dm}^3 \text{ mol}^{-1} \text{ cm}^{-1}$  (514 nm) and  $36,400 \text{ dm}^3 \text{ mol}^{-1} \text{ cm}^{-1}$  (519 nm), respectively. These numbers are obviously larger than that of N719, indicating good light-harvesting ability. Although PS and CP1 have the similar absorption maxima ( $\lambda_{\max}$ ) and molar extinction coefficients, CP1 has broader absorption range than PS does. These results suggest that the absorption spectrum is determined by both the length of the conjugated linker and the nature of the donor group.

To further study the mechanism of electron injection from the dye to conduction band (CB) of semiconductor, followed by the reduction of the dye cation back to its original state for the next

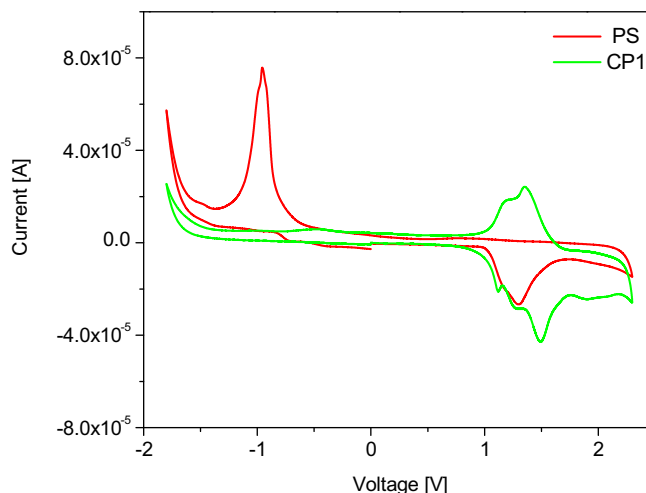


Figure 3. The CV curves of dyes in  $\text{CH}_2\text{Cl}_2$ .

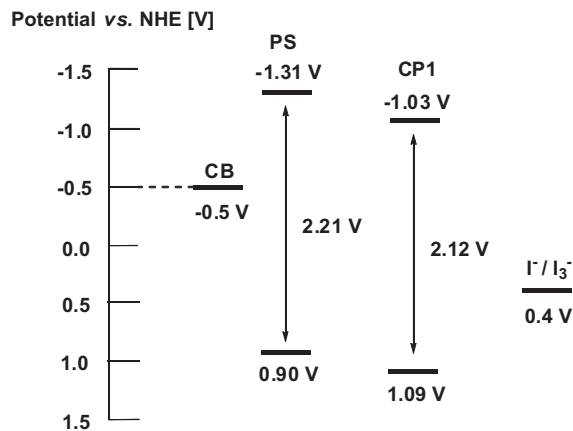


Figure 4. Molecular orbital energy diagram of HOMO and LUMO of dyes.

cycle, the CVs of these dyes were performed in  $\text{CH}_2\text{Cl}_2$  to measure the redox potentials (Fig. 3). The first oxidation potentials ( $E_{\text{ox}}$ ) corresponding to the HOMO energy levels of the dyes were summarized in Table 1. The HOMO energy levels of PS and CP1 dyes are 0.90 and 1.09 V, respectively. These values are higher than that of iodine/iodide (0.4 V)<sup>22</sup>, therefore the oxidized dyes could be reduced effectively by electrolyte and regenerated (Fig. 4). The LUMO energy levels of these dyes can be calculated by using HOMO energy level and zeroth-zeroth energy ( $E_{0-0}$ ) of the dyes estimated from the intersection between the absorption and emission spectra, namely, HOMO- $E_{0-0}$ . To effectively inject the electron into the CB of  $\text{TiO}_2$ , the LUMO energy levels of the dyes must be much lower than the conducting band energy ( $E_{\text{cb}}$ ) of the semiconductor,

**Table 2**  
Photovoltaic performance of DSSCs based on PS, CP1 and N719 dyes<sup>a</sup>

Dye	$J_{sc}/\text{mA cm}^{-2}$	$V_{oc}/\text{V}$	Fill factor	$\eta$ (%)
PS <sup>b</sup>	0.75	0.56	0.63	0.26
CP1 <sup>b</sup>	7.84	0.66	0.67	3.47
N719 <sup>c</sup>	10.43	0.76	0.66	5.27

<sup>a</sup> Measured under irradiation of AM 1.5G simulated solar light ( $100 \text{ mW cm}^{-2}$ ) at room temperature,  $12 \mu\text{m}$  film thickness,  $0.25 \text{ cm}^2$  working area; electrolyte: 1.0 M 1,2-dimethyl-3-*n*-propylimidazolium iodide (DMPII), 0.05 M LiI, 0.03 M  $\text{I}_2$ , 0.1 M guanidinium thiocyanate (GuSCN), 0.5 M 4-*tert*-butylpyridine (TBP) in AcCN and valeronitrile (85:15).

<sup>b</sup> The concentration of pyridinium dyes are  $3 \times 10^{-4} \text{ M}$  in  $\text{CH}_2\text{Cl}_2$ .

<sup>c</sup> The concentration of N719 dye is  $3 \times 10^{-4} \text{ M}$  in ethanol.

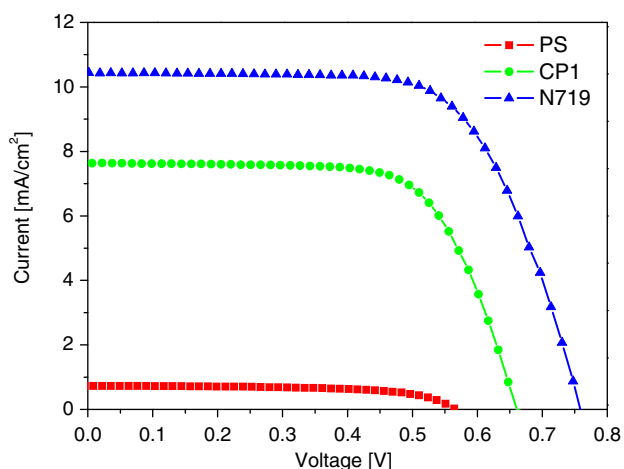


**Figure 5a.** Photocurrent density versus voltage curves for DSSCs based on PS, CP1 and N719 under irradiation of AM 1.5G simulated solar light ( $100 \text{ mW cm}^{-2}$ ).

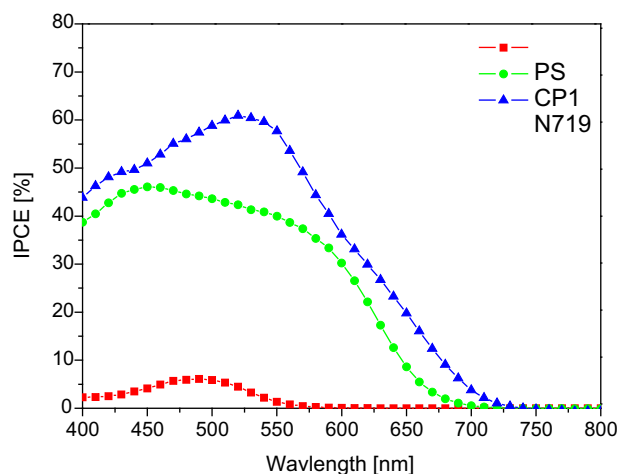


**Figure 5b.** The incident photon-to-current conversion efficiencies spectra for DSSCs based on PS, CP1 and N719.

–0.5 V (vs NHE). Both of the dyes can achieve the electron injection and form the oxidized dyes according to their LUMO energy values (Fig. 4). The relatively large energy gaps between the LUMO of the dyes and  $E_{cb}$  of semiconductor are sufficient for efficient electron injection.

The photovoltaic properties of these dyes on DSSCs are shown in Table 2 and  $J$ – $V$  curves of the dyes are shown in Fig. 5a. We have achieved a  $\eta$  value of 0.26% (with short-circuit photo current density  $J_{sc} = 0.75 \text{ mA/cm}^2$ , open circuit photovoltage  $V_{oc} = 0.56 \text{ V}$ , and fill factor  $ff = 0.63$ ) and 3.47% (with short-circuit photo current

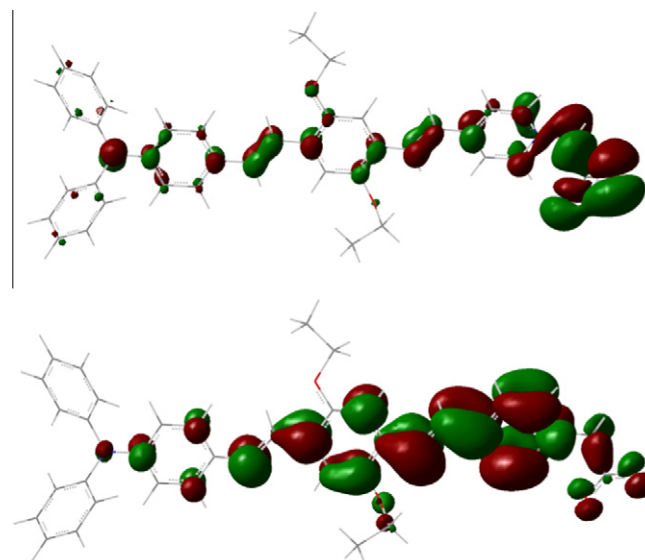


**Figure 6.** The frontier molecular orbitals (MOs) of the HOMO (top) and LUMO (bottom) of the CP1 dye.

density  $J_{sc} = 7.84 \text{ mA/cm}^2$ , open circuit photovoltage  $V_{oc} = 0.66 \text{ V}$ , and fill factor  $ff = 0.67$ ) for DSSCs using PS and CP1, respectively. Under the similar conditions, the N719 dye gives a  $\eta$  value of 5.27%. The fill factor ( $ff$ ) of CP1 is similar to those of PS and N719. However, CP1 gives much higher  $J_{sc}$  and  $V_{oc}$  than the hemicyanine dye PS does. Noticeably, most hemicyanine dyes have lower  $V_{oc}$  around 0.40–0.60 V, than that of CP1 (up to 0.66 V). The incident photon-to-current conversion efficiencies (IPCEs) of these dyes in DSSCs are shown in Figure 5b. CP1 gives higher IPCE value and broader IPCE spectrum than PS does in the spectral range of 400–700 nm, with highest value of 46% at 450 nm. Compared with N719, CP1 has lower  $J_{sc}$ , which might be resulted from the fact that the methylene group in the pyridinium framework disrupts the  $\pi$ -conjugation between the pyridinium and the carboxylate, thus decreases the electron injection efficiency in a dynamic manner.<sup>23</sup>

Density functional theory (DFT) calculations were performed at a B3LYP/3-21G (d) level for the geometry optimization to observe frontier molecular orbitals (MOs) of the HOMO and LUMO. The frontier MOs of the CP1 reveal that HOMO–LUMO excitation moves the electron density distribution from TPA moieties to the N-substituted pyridinium (Fig. 6). It is noteworthy that the LUMO electron density of the CP1 is located mainly on the N-substituted pyridinium, therefore the excited electron can be injected into the  $\text{TiO}_2$  electrode efficiently.

In summary, we have synthesized a new pyridinium hemicyanine dye CP1 for DSSCs. A prominent solar energy-to-electricity conversion efficiency ( $\eta$ ) of 3.47% and high  $V_{oc}$  are achieved in a DSSC using this dye. CP1 is simple in structure, easy to synthesize, and has good DSSC performance. Further structural modification to improve the DSSC performance is in progress.

## Acknowledgments

We gratefully acknowledge the financial support of this work from Shanghai Committee of Science and Technology of China (Grant No. 10520710100). We also thank the Laboratory of organic Functional molecules, Sino-French Institute of ECNU for support.

## Supplementary data

Supplementary data associated with this article can be found, in the online version, at doi:10.1016/j.tetlet.2011.12.133.

## References and notes

1. O'Regan, B.; Grätzel, M. *Nature* **1991**, 353, 737–740.
2. Nazeeruddin, M. K.; Kay, A.; Rodicio, I.; Humphry-Baker, R.; Müller, E.; Liska, P.; Vlachopoulos, N.; Grätzel, M. *J. Am. Chem. Soc.* **1993**, 115, 6382–6390.
3. Nazeeruddin, M. K.; Zakeeruddin, S. M.; Humphry-Baker, R.; Jirousek, M.; Liska, P.; Vlachopoulos, N.; Grätzel, M. *Inorg. Chem.* **1999**, 38, 6298–6305.
4. Nazeeruddin, M. K.; Péchy, P.; Renouard, T.; Zakeeruddin, S. M.; Humphry-Baker, R.; Comte, P.; Liska, P.; Cevey, L.; Costa, E.; Shklover, V.; Spiccia, L.; Deacon, G. B.; Bignozzi, C. A.; Grätzel, M. *J. Am. Chem. Soc.* **2001**, 123, 1613–1624.
5. Gao, F.; Wang, Y.; Shi, D.; Zhang, J.; Wang, M.; Jing, X. *J. Am. Chem. Soc.* **2008**, 130, 10720–10728.
6. Cao, Y. M.; Bai, Y.; Yu, Q. J.; Cheng, Y. M.; Liu, S.; Shi, D. *J. Phys. Chem. C* **2009**, 113, 6290–6297.
7. Chen, C. Y.; Wu, S. J.; Wu, C. G.; Chen, J. G.; Ho, K. C. *Angew. Chem., Int. Ed.* **2006**, 45, 5822–5825.
8. Hara, K.; Sayama, K.; Ohga, Y.; Shinpo, A.; Suga, S.; Arakawa, H. *Chem. Commun.* **2001**, 6, 569–570.
9. Hara, K.; Wang, Z.; Sato, T.; Furube, A.; Katoh, R.; Sugihara, H. *J. Phys. Chem. B* **2005**, 109, 5476–5482.
10. Wang, Z. S.; Li, F. Y.; Huang, C. H.; Wang, L.; Wei, M.; Jin, L. P. *J. Phys. Chem. B* **2000**, 104, 9676–9682.
11. Wang, Z.; Li, F.; Huang, C. *Chem. Commun.* **2000**, 2063–2064.
12. Horiuchi, T.; Miura, H.; Sumioka, K.; Uchida, S. *J. Am. Chem. Soc.* **2004**, 126, 12218–12219.
13. Ito, S.; Miura, H.; Uchida, S.; Takata, M.; Sumioka, K.; Liska, P. *Chem. Commun.* **2008**, 41, 5194–5196.
14. Liu, B.; Zhu, W.; Zhang, Q.; Wu, W.; Xu, M.; Ning, Z.; Xie, Y.; Tian, H. *Chem. Commun.* **2009**, 13, 1766–1768.
15. Sayama, K.; Hara, K.; Mori, N.; Satsuki, M.; Suga, S.; Tsukagoshi, S. *Chem. Commun.* **2000**, 1173–1174.
16. Tian, H.; Yang, X.; Chen, R.; Zhang, R.; Hagfeldt, A.; Sun, L. C. *J. Phys. Chem. C* **2008**, 112, 11023–11033.
17. Zeng, W. D.; Cao, Y. M.; Bai, Y.; Wang, Y. H.; Shi, Y. S.; Wang, P. *Chem. Mater.* **2010**, 22, 1915–1925.
18. Li, G.; Zhou, Y.; Cao, X.; Bao, P.; Jiang, K.; Lin, Y. *Chem. Commun.* **2009**, 16, 2201–2203.
19. Hagberg, D. P.; Yum, J. H.; Lee, H. J.; Angelis, F. D.; Marinado, T.; Karlsson, K. M. *J. Am. Chem. Soc.* **2008**, 130, 6259–6266.
20. Ooyama, Y.; Harima, Y. *Eur. J. Org. Chem.* **2009**, 2903–2934.
21. Chen, Y. S.; Li, C.; Zeng, Z. H.; Wang, W. B.; Wang, X. S.; Zhang, B. W. *J. Mater. Chem.* **2005**, 15, 1654–1661.
22. Hagfeldt, A.; Grätzel, M. *Chem. Rev.* **1995**, 95, 49–68.
23. Satoh, N.; Nakashima, T.; Yamamoto, K. *J. Am. Chem. Soc.* **2005**, 127, 13030–13038.
24. Yella, A.; Lee, H.; Tsao, H. N.; Yi, C.; Chandiran, A. K.; Nazeeruddin, M. K.; Diau, E. W.; Yeh, C.; Zakeeruddin, S. M.; Grätzel, M. *Science* **2011**, 334, 629–634.